BRIEF COMMUNICATION
https://doi.org/10.1038/s41564-022-01092-1

nature microbiology

Differential neutralizing antibody responses elicited by CoronaVac and BNT162b2 against SARS-CoV-2 Lambda in Chile

Mónica L. Acevedo[1,2,11], Aracelly Gaete-Argel[1,11], Luis Alonso-Palomares[1], Marco Montes de Oca[3], Andrés Bustamante[1], Aldo Gaggero[4], Fabio Paredes[5], Claudia P. Cortes[2,6,7], Sergio Pantano[8], Constanza Martínez-Valdebenito[9,10], Jenniffer Angulo[9,10], Nicole Le Corre[9,10], Marcela Ferrés[9,10], Marcelo A. Navarrete[3], Fernando Valiente-Echeverría[1,2] ✉ and Ricardo Soto-Rifo[1,2] ✉

SARS-CoV-2 variant Lambda was dominant in several South American countries, including Chile. To ascertain the efficacy of local vaccination efforts, we used pseudotyped viruses to characterize the neutralization capacity of antibodies elicited by CoronaVac ($n = 53$) and BNT162b2 ($n = 56$) in healthcare workers from Clínica Santa María and the Faculty of Medicine at Universidad de Chile, as well as in convalescent plasma from individuals infected during the first wave visiting the Hospital Clínico at Pontificia Universidad Católica ($n = 30$). We observed that BNT162b2 elicits higher neutralizing antibody titres than CoronaVac, with differences ranging from 7.4-fold for the ancestral spike (Wuhan-Hu-1) to 8.2-fold for the Lambda spike and 13-fold for the Delta spike. Compared with the ancestral virus, neutralization against D614G, Alpha, Gamma, Lambda and Delta variants was reduced by between 0.93- and 4.22-fold for CoronaVac, 1.04- and 2.38-fold for BNT162b2, and 1.26- and 2.67-fold for convalescent plasma. Comparative analyses among the spike structures of the different variants suggest that mutations in the spike protein from the Lambda variant, including the 246–252 deletion in an antigenic supersite at the N-terminal domain loop and L452Q/F490S within the receptor-binding domain, may account for immune escape. Interestingly, analyses using pseudotyped and whole viruses showed increased entry rates into HEK293T-ACE2 cells, but reduced replication rates in Vero-E6 cells for the Lambda variant when compared with the Alpha, Gamma and Delta variants. Our data show that inactivated virus and messenger RNA vaccines elicit different levels of neutralizing antibodies with different potency to neutralize SARS-CoV-2 variants, including the variant of interest Lambda.

The emergence of SARS-CoV-2 variants of concern (VOC) and interest (VOI) has been a hallmark of the COVID-19 pandemic during 2021[1,2]. Classification of VOC and VOI by the World Health Organization has been highly dynamic with emergent SARS-CoV-2 variants such as Lambda (lineage C.37), Delta (lineage B.1.617.2), Mu (lineage B.1.621) and Omicron (B.1.1.529) being the most recently recognized, whereas others such as Epsilon (lineage B.1.427/29), Zeta (lineage P.2) and Theta (lineage P.3) are no longer considered as VOI[3]. VOC and VOI are characterized by the presence of mutations located in key positions of the spike protein, including those in the receptor-binding domain (RBD) such as N501Y (shared by VOC Alpha, Beta, Gamma and Omicron) associated with increased Angiotensin-Converting Enzyme 2 (ACE2) binding and infectivity, or K417N/T and E484K/A (shared by VOC Beta, Gamma and Omicron) associated with escape from neutralizing antibodies[1]. The spike protein of VOI Lambda, responsible for major outbreaks in South American countries, including Chile, has a pattern of seven mutations (G75V, T76I, Δ246–252, L452Q, F490S, D614G, T859N) of which L452Q is similar to the L452R mutation reported in the Delta and Epsilon variants[4].

The presence of mutations in antigenic sites characteristic of SARS-CoV-2 VOC and VOI has raised concerns regarding their impact on the neutralizing capacity of antibodies elicited by currently available vaccines, which were designed using the ancestral spike as a reference. Indeed, several studies have shown that VOC and VOI escape neutralization from antibodies elicited by vaccines, although to different extents[1]. Interestingly, recent studies suggested that neutralizing antibody titres elicited by vaccines should be considered as a correlate of protection[5–9]. As such, the emergence of SARS-CoV-2 variants carrying mutations in antigenic sites within the spike protein and their impact on neutralization by antibodies elicited by vaccines requires continuous monitoring.

The virus-inactivated vaccine CoronaVac and the messenger RNA vaccine BNT162b2 are the most widely inoculated vaccines worldwide and were identified among those with lower and higher correlates of protection, respectively[5,6,10]. Therefore, we sought to determine and compare the neutralization capacity of plasma samples obtained from 109 healthcare workers from Clínica Santa María and the Faculty of Medicine at Universidad de Chile, both in Santiago, Chile, receiving the complete scheme of these vaccines during the Chilean Ministry of Health's vaccination campaign (Supplementary Table 1).

[1]Laboratorio de Virología Molecular y Celular, Programa de Virología, Instituto de Ciencias Biomédicas, Universidad de Chile, Santiago, Chile. [2]Millennium Institute on Immunology and Immunotherapy, Santiago, Chile. [3]Escuela de Medicina, Universidad de Magallanes, Punta Arenas, Chile. [4]Laboratorio de Virología Ambiental, Programa de Virología, Instituto de Ciencias Biomédicas, Universidad de Chile, Santiago, Chile. [5]Departamento de Epidemiología, Ministerio de Salud de Chile, Santiago, Chile. [6]Clínica Santa María, Santiago, Chile. [7]Departamento de Medicina Centro, Universidad de Chile, Santiago, Chile. [8]Biomolecular Simulations Group, Instituto Pasteur de Montevideo, Montevideo, Uruguay. [9]Departamento de Enfermedades Infecciosas e Inmunología Pediátricas, División de Pediatría, Escuela de Medicina, Pontificia Universidad Católica de Chile, Santiago, Chile. [10]Laboratorio de Infectología y Virología Molecular, Laboratorio de Bioseguridad Nivel 3, Escuela de Medicina, Pontificia Universidad Católica de Chile, Santiago, Chile. [11]These authors contributed equally: Mónica L. Acevedo, Aracelly Gaete-Argel. ✉e-mail: fvaliente@uchile.cl; rsotorifo@uchile.cl

We generated pseudotyped viruses carrying either the ancestral SARS-CoV-2 spike protein (Wuhan-Hu-1; lineage A)[11], the spike protein carrying the D614G mutation (lineage B.1) or the spike from variants Alpha (lineage B.1.1.7), Gamma (lineage P.1), Lambda (lineage C.37) and Delta (lineage B.1.617.2). These variants have dominated the COVID-19 pandemic in Chile during 2021 (Extended Data Fig. 1a,b). Neutralization assays using the pseudotyped virus carrying the ancestral spike revealed that the geometric mean of the pseudotyped virus neutralization titre 50 ($pVNT_{50}$) was 97.78 (95% confidence intervals (CI) 71.51 to 133.7) for individuals receiving the inactivated virus vaccine, and 720 (95% CI 567.2 to 913.9) for those inoculated with the mRNA vaccine (Fig. 1a and Supplementary Tables 2 and 3). These data indicate that the BNT162b2 vaccine elicits 7.4-fold higher neutralizing antibody titres against the ancestral spike protein compared with CoronaVac (Fig. 1a). Neutralization assays using pseudotypes carrying the D614G mutant or the Alpha, Gamma, Lambda and Delta variants resulted in geometric mean $pVNT_{50}$ values of 104.9 (95% CI 78.9 to 139.5), 60.31 (95% CI 42.51 to 85.56), 58.27 (95% CI 40.05 to 84.79), 47.43 (95% CI 34.41 to 65.38) and 23.15 (95% CI 16.98 to 31.56), respectively, for the CoronaVac samples, and 692 (95% CI 560.6 to 854.6), 466 (95% CI 368.2 to 589.8), 389.7 (95% CI 301.6 to 503.7), 309.5 (95% CI 311.6 to 489.4) and 301.7 (95% CI 230.5 to 394.9) for the BNT162b2 samples (Fig. 1b and Supplementary Tables 2 and 3). Neutralizing antibody titres against spike variants were 6.6- to 13-fold higher for BNT162b2 vaccinees (Fig. 1b). Compared with the ancestral spike, neutralizing antibody titres elicited by CoronaVac decreased by a factor of 0.9 for the D614G mutant, 1.6 for the Alpha spike, 1.7 for the Gamma spike, 2.1 for the Lambda spike and 4.2 for the Delta spike (Fig. 1c,d and Supplementary Tables 2 and 3). Neutralizing antibody titres elicited by BNT162b2 decreased by a factor of 1.04, 1.54, 1.84, 1.84 and 2.38 for the D614G mutant or the Alpha, Gamma, Lambda and Delta variants, respectively (Fig. 1e,f and Supplementary Tables 2 and 3).

Demographic analyses of our vaccinated cohort regarding sex, age, body mass index (BMI) or smoking status and neutralizing antibody titres showed positive correlations between age-CoronaVac-NAbs and Delta ($P=0.0221$), age-BNT162b2-NAbs and D614G ($P=0.0285$) and BMI-BNT162b2-NAbs and Delta ($P=0.025$) (Extended Data Fig. 2a,d).

We also performed neutralization analyses using 30 samples from convalescent individuals infected during the first wave in Chile. This wave was dominated by the B.1 lineage and occurred before the circulation of SARS-CoV-2 variants in the country and the use of vaccines (Extended Data Fig. 3). Here geometric means of $pVNT_{50}$ were 454.8 (95% CI 351.3 to 588.8), 361.4 (95% CI 251.6 to 519.1), 270.5 (95% CI 180.6 to 405.1), 208.4 (95% CI 145.7 to 298.1), 195.2 (95% CI 132.9 to 286.8) and 169.8 (95% CI 108 to 267.1) for ancestral lineage, D614G, Alpha, Gamma, Lambda and Delta, respectively. As such, neutralizing antibody titres were decreased by a factor of 1.26, 1.68, 2.18, 2.33 and 2.67 for D614G, Alpha, Gamma, Lambda and Delta, respectively (Extended Data Fig. 3 and Supplementary Table 4).

Comparative analyses of immunogenic regions showed that the four tested SARS-CoV-2 variants display mutations in immunodominant epitopes of the receptor-binding motif targeted by class I and class II antibodies (Extended Data Fig. 4a,b). Whereas Alpha and Gamma carry a polar to aromatic change (N501Y), and Gamma changes the charge of hydrophilic amino acids (E484K, K417T) in the receptor-binding motif within the RBD, the Delta variant carries the L452R mutation shown to confer both increased infectivity and escape from neutralizing antibodies[12,13]. The Lambda RBD variant carries the L452Q mutation that is similar to the L452R mutation described in Delta, and the F490S mutation, which has also been associated with escape from neutralizing antibodies[12,14]. On the other hand, all tested variants show substitutions in the N-terminal domain (NTD) antigenic supersite. However, whereas the Alpha variant carries a single amino acid deletion (ΔY144) in the β-hairpin, and Gamma displays two substitutions in the N terminus (L18F, T20N), the Lambda variant harbours a seven amino acid deletion of the supersite loop (Δ246–252) described as an antigenic supersite[15]. Indeed, both L452Q/F490S and Δ246–252 reside at the interface between the spike protein and monoclonal antibodies targeting the RBD and the NTD, respectively (Extended Data Fig. 5a,b). By contrast, the Delta variant shows changes at the N terminus (T19R) and in the β-hairpin (Δ156–157, R158G). This distinctive substitution pattern within antigenic sites may, at least in part, explain the different neutralizing activity of CoronaVac and BNT162b2-induced polyvalent sera against the tested variants.

Analyses using equivalent amounts of pseudotyped viruses in previously described HEK293T-ACE2 cells[11], showed that the Lambda spike provides increased viral entry when compared with Alpha, Gamma and Delta spikes (Fig. 2a). However, viral replication assays using equivalent viral titres (multiplicity of infection (MOI) = 1) to infect Vero-E6 cells showed that Lambda replicates at lower rates compared with the Alpha, Gamma and Delta variants, as indicated by a significant higher cycle threshold value (which is inversely related to viral RNA levels) in the released genomic RNA recovered both at 24 and 48 hours post infection (Fig. 2b). Although some RBD mutations such as N501Y and L452R have been linked to increased infectivity[1,12,13], mutations within intermediate folding domains may also change infectivity by affecting the spike molecular dynamics[16,17]. In this sense, the spike protein of the Lambda variant displays the substitution T859N that lies in the neighbourhood of G614 in the apposed protomer (Extended Data Fig. 6a). In the ancestral spike protein, the D614–T859 interaction was proposed to modulate the stability of the inter-protomer interface, and earlier molecular dynamics simulations suggest that fluctuations in the native contacts may facilitate transition between up and down states in the spike's RBD[18]. In fact, the G614 form increases the occupancy of the one-up state, which accounts for its enhanced infectivity[19]. We also noticed that T859 forms hydrophobic contacts with F592 in the apposed protomer (Extended Data Fig. 6a). Interestingly, conservation analysis among betacoronavirus spikes revealed that when a phenylalanine is present at an equivalent 592 position, it is coupled to threonine at 859 exclusively in the sarbecovirus group, which includes SARS-CoV, PCoV (pangolin), RatG13 (bat) and SARS-CoV-2 (Extended Data Fig. 6b). Interestingly, we were not able to observe differences between pseudotyped viruses carrying the Lambda spike and the original residue (T859) or the T859N

Fig. 1 | Neutralization titres of plasma from individuals receiving CoronaVac and BNT162b2 vaccines. a,**b**, $pVNT_{50}$ of recipients of the CoronaVac vaccine ($n=53$) and of the BNT162b2 vaccine ($n=56$) against (**a**) pseudotype Wuhan-Hu-1 reference strain (wild-type) or (**b**) D614G (B.1), Alpha (B.1.1.7), Gamma (P.1), Lambda (C.37) and Delta (B.1.617.2) variants. The statistical significance of the difference between the neutralization was calculated by Wilcoxon matched-pairs signed-rank test. Two-tailed *P* values are reported. Geometric mean titres and 95% CIs are indicated. **c**,**d**, Box plots indicate the median and interquartile range of $pVNT_{50}$ for each SARS-CoV-2 pseudotype for the CoronaVac (**c**) and BNT162b2 (**d**) groups. Factor changes are shown in parentheses as the difference of the geometric mean titre in $pVNT_{50}$ compared with that of the wild-type pseudotyped virus. Statistical analyses were performed with the two-tailed Kruskal–Wallis test after adjustment for the false discovery rate. Geometric mean titres are indicated. **e**,**f**, Results are shown as the difference in neutralization titres of matched samples for each SARS-CoV-2 pseudotype in the CoronaVac (**e**) and BNT162b2 (**f**) groups. *P* values for comparison of the $pVNT_{50}$ were calculated with the Wilcoxon signed-rank test.

mutation (Fig. 2c). Considering the presence of the T859N mutation in several SARS-CoV-2 lineages, its effects on neutralization by antibodies warrant further investigation.

The data presented here confirm that neutralizing antibody titres elicited by the mRNA vaccine BNT162b2 are higher than those elicited by the inactivated virus vaccine CoronaVac in a real-life

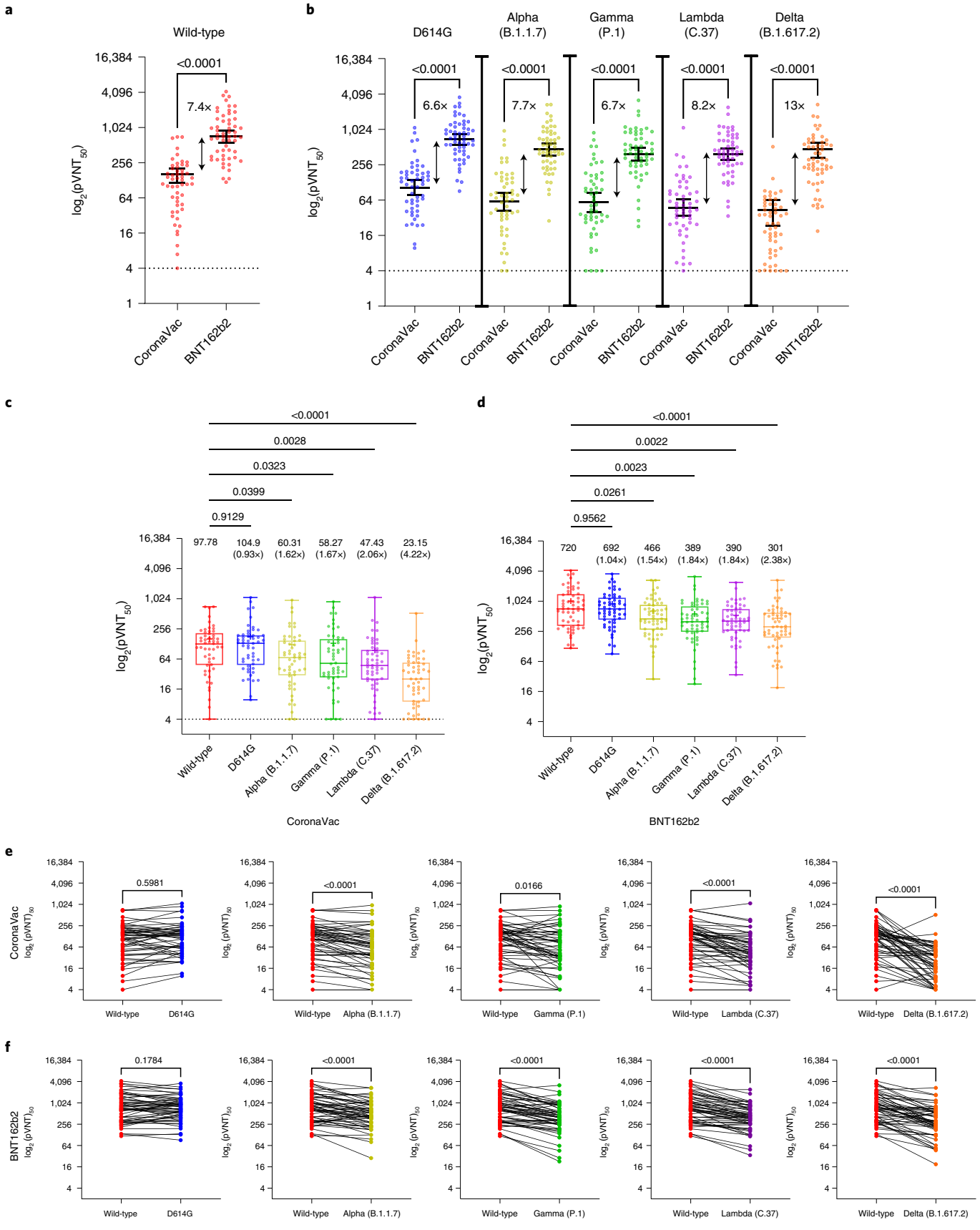

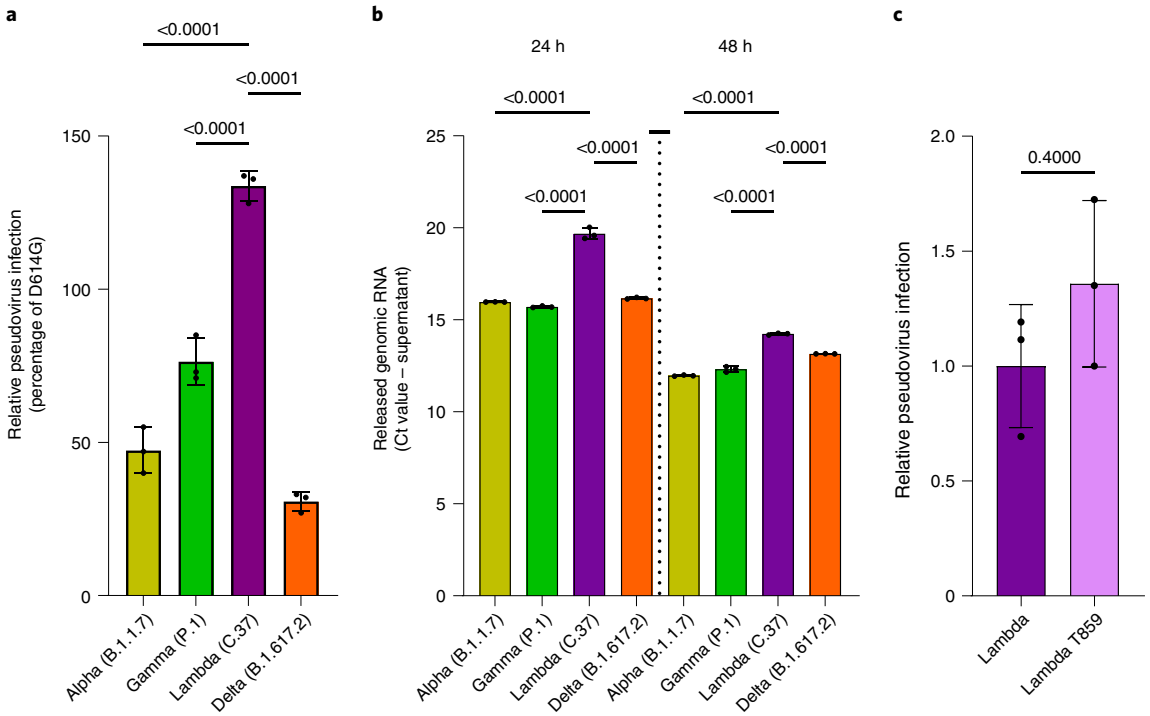

Fig. 2 | Infectivity and replication of SARS-CoV-2 variant Lambda. a, Levels of infection of SARS-CoV-2 pseudotypes bearing the Alpha (B.1.1.7), Gamma (P.1), Lambda (C.37) and Delta (B.1.617.2) spike protein in HEK293T cells stably expressing ACE2. Cells were seeded in 96-well plates and infected with 0.5 RT units of the indicated pseudotyped viruses for 48 h. Two biological replicates were assessed in three independent experiments. Data are presented as the mean ± s.d. of three independent experiments. *P* values were determined by ANOVA. **b**, Genomic RNA levels Alpha, Gamma, Lambda and Delta viruses produced on infection of Vero-E6 cells. Cells were infected at a MOI = 1. Genomic RNA levels are expressed as cycle threshold (Ct) values, which are inversely related to viral load. Data are presented as the mean ± s.d. of three experiments. *P* values were determined by ANOVA from a sample size of $n = 3$. **c**, Levels of infection of SARS-CoV-2 pseudotypes bearing the Lambda (C.37) and Lambda mutant T859 spike protein in HEK293T-ACE2 cells. Cells were seeded in 96-well plates and infected with 0.5 RT units of the indicated pseudotyped viruses for 48 h. Two biological replicates were assessed in three independent experiments. Data are presented as the mean ± s.d. of three independent experiments. *P* values were determined by Mann–Whitney signed-ranked test.

vaccination setting. Previous studies have shown that most of the neutralizing antibodies are directed to antigenic sites present in the RBD and, to a lesser extent, antigenic sites in the NTD[1,2]. In this sense, BNT162b2 delivers an mRNA sequence encoding a spike protein stabilized in the prefusion conformation that keeps intact the RBD and NTD-containing S1 domain[20]. Conversely, studies performed on a β-propiolactone inactivated virus like that used in the CoronaVac vaccine showed that 74.4% of the spike proteins are in the post-fusion conformation. Thus, a minor fraction (25.6%) of the spike proteins has the major antigenic sites present in the S1 domain[21]. Moreover, treatment of SARS-CoV-2 particles with β-propiolactone may induce virus aggregation, diminishing its antigenic capacity[22]. These differences in the availability of antigenic sites may explain, at least in part, the differences in the neutralizing antibody titres observed between both vaccine platforms.

Interestingly, a nationwide study for BNT162b2 effectiveness in Israel revealed that this vaccine was 97% efficient in preventing symptomatic COVID-19, 97.5% efficient against severe or critical disease and 96.7% efficient in preventing COVID-19-related deaths[23]. A similar study for CoronaVac performed in Chile showed that this vaccine was 65.9% efficient in preventing COVID-19, 90.3% efficient in preventing intensive care unit admission and 86.3% efficient in preventing COVID-19-related deaths[24]. The differences observed in the neutralizing antibody titres elicited by these two vaccines and the ability of these antibodies to neutralize SARS-CoV-2 variants may help to explain the differences observed, especially those relating to their effectiveness to prevent symptomatic disease (97% for BNT162b2 versus 65.9% for CoronaVac) in a real-life vaccination setting involving millions of individuals. Therefore, our data provide further evidence favouring the use of neutralizing antibody titres as a correlate of protection, as recently suggested[5–9]. The implementation of a correlate of protection is critical when analysing the impact of emerging SARS-CoV-2 variants such as Mu, Delta and now, Omicron.

The data presented here also show that the unique pattern of mutations present in the spike protein of VOI Lambda confers escape from neutralizing antibodies elicited by CoronaVac, BNT162b2 and convalescent plasma, which is in agreement with recent observations[25]. The escape by Lambda from neutralizing antibodies was higher than that observed for Alpha and Gamma variants, but lower than that observed for Delta, indicating that escape from neutralizing antibodies is a key feature of this globally dominant variant. Because the 246–252 deletion in the NTD and the L452Q/F490S mutations in the RBD of the Lambda spike are located in antigenic sites, these mutations may reduce the affinity of neutralizing antibodies. Our data also suggest that the unique set of spike mutations present in the Lambda variant confer increased viral entry, but that the replication fitness is lower compared with other variants. Together, these observations may help explain the rapid rise and high circulation rates of the Lambda variant in South American countries before emergence of the Delta variant.

Methods

Study cohort. Healthcare workers without previously diagnosed SARS-CoV-2 infection from Clínica Santa María and the Faculty of Medicine at Universidad de Chile, both in Santiago, Chile, were invited to participate. Volunteers received the

two-dose scheme of CoronaVac or BNT162b2, each dose being administered 28 or 21 d apart, respectively, according to the Chilean vaccination programme. Plasma samples were collected between May and June 2021. Convalescent individuals were participating in the study COVID0920 carried out at Hospital Clínico Red de Salud UC Christus, Santiago, Chile. All participants signed an informed consent before any study procedure was undertaken.

Pseudotype infectivity assay. Pseudotyped viruses carrying different SARS-CoV-2 spike proteins were prepared as previously described[11]. Briefly, HIV-1-based SARS-CoV-2 pseudotypes were produced in HEK293T cells by transfecting the pNL4.3-ΔEnv-Luc together with the corresponding pCDNA-SARS-CoV-2 Spike coding vector in a 1:1 molar ratio. Plasmids coding a codon-optimized spike lacking the last 19 amino acids of the C-terminal end (SΔ19) known to avoid retention at the endoplasmic reticulum were obtained by gene synthesis or customized site-directed mutagenesis (GeneScript). They contained the following mutations: lineage A (reference sequence), lineage B (D614G), lineage B.1.1.7 (Δ69–70, Δ144, N501Y, A570D, D614G, P681H, T716I, S982A, D1118H), lineage P.1 (L18F, T20N, P26S, D138Y, R190S, K417T, E484K, N501Y, D614G, H655Y, T1027I), lineage C.37 (G75V, T76I, Δ246–252, L452Q, F490S, D614G, T859N) and lineage B.1.617.2 (T19R, del157/158, L452R, T478K, D614G, P681R, D950N). Each pseudotype preparation was cleared by centrifugation at 850*g* at room temperature, quantified using the HIV-1 Gag p24 Quantikine ELISA Kit (R&D Systems) or the EnzChek Reverse Transcriptase Assay (ThermoFisher Scientific), aliquoted in 50% fetal bovine serum (FBS; Sigma-Aldrich) and stored at −80 °C until use.

Different amounts of pseudotyped viruses (as determined by the levels of the HIV-1 p24 protein) were used to infect HEK-ACE2 cells, and 48 h later, firefly luciferase activity was measured using the Luciferase Assay Reagent (Promega) in a Glomax 96 Microplate luminometer (Promega).

SARS-CoV-2 variants isolation and infectivity assay. Vero-E6 cells (African green monkey) were maintained in DMEM (low glucose) containing 10% FBS, 1% antibiotics (penicillin and streptomycin) in a 5% CO_2 atmosphere. Five isolates belonging to B.1.1 (D614G), P.1 (Gamma), B 1.1.7 (Alpha), C.37 (Lambda) and B.1.617.2 (Delta) were isolated from SARS-CoV-2-positive subjects and inoculated into Vero-E6 in a biosafety level 3 laboratory. Virus supernatants were harvested and sequenced using the ARTIC SARS-CoV-2 ONT (Oxford Nanopore Technologies) sequencing protocol; vials were stored at −80 °C and the viral titre was measured by plaque assay.

For infectivity assay, Vero-E6 cells were seeded in two 24-well plates at 80% confluence and, after 24 h, an MOI of 1 for each variant was inoculated in triplicate into cells. After, 1 h at 37 °C and 5% CO_2, the inoculum was removed and monolayers were replenished with DMEM supplemented with 2% FBS and 1% antibiotics (penicillin and streptomycin). Supernatants (200 µl) were collected at 24 and 48 h post inoculation and mixed with 200 µl of lysis buffer before PCR with reverse transcription assay. The PCR with reverse transcription assay was carried out with LightMix from TibMolBiol (Roche) against RdRP and the crossing threshold of each variant was normalized with the crossing threshold of each initial inoculum.

Neutralization assay. Plasma samples inactivated for 30 min at 56 °C were threefold serially diluted (from 1:2 to 1:4,374 for the CoronaVac group, from 1:5 to 1:10,935 for the BNT162b2 group and from 1:20 to 1:43,740 for the convalescent plasma) in supplemented DMEM. In parallel, pseudoviruses were thawed on ice and diluted to equal the p24 concentration in DMEM 50% FBS. A subsequent dilution of pseudovirus was prepared in supplemented DMEM to obtain 3 ng of p24 in 50 µl. Then, 50 µl of sample dilutions were mixed with 50 µl of each variant pseudovirus in duplicate and the mixture was incubated for 1 h at 37 °C. Later, 1×10^4 HEK-ACE2 cells in 100 µl of supplemented DMEM were added to each well and HEK293T cells transduced with the wild-type (lineage A) pseudovirus were used as a control. Cells were lysed 48 h later, and firefly luciferase activity was measured using the Luciferase Assay Reagent (Promega) in a Glomax 96 Microplate luminometer (Promega).

Relative luminescence units (RLUs) of HEK293T cells transduced with wild-type pseudovirus were averaged and considered as 100% neutralization, whereas RLUs measured at the highest dilution of each sample were established as 0% neutralization. Thus, the percentage of neutralization of each one of the eight dilutions of a sample was calculated as the complement of the division between the corresponding RLUs and the RLUs obtained at the higher dilution after subtracting the background (HEK293T cells plus wild-type pseudotyped virus). This calculation was done independently for each technical replicate and each spike variant.

Pseudotyped virus-neutralizing antibody titre (ID_{50}) was calculated in GraphPad Prism v.9.2.0 by modelling a four-parameter nonlinear regression with variable slope constraining top values to 100 and bottom values to 0. Samples showing an ID_{50} lower than the first dilution (1:4 for CoronaVac, 1:10 for BNT162b2 or 1:40 for convalescent plasma) were considered as 4, 10 or 40, respectively.

Spike protein and sequence analyses. Mutations and antigenic sites were mapped on previously determined crystal structures (PDB: 7BNN, PDB: 7BWJ, PDB: 7LY0). Structural alignments were performed using Swiss-PdbViewer, displayed by PyMOL v.2.4.1 (http://www.pymol.org/pymol), and rendered by Blender v.2.92.0 (http://www.blender.org). The reference sequence of spike protein included in the analysis was YP_009724390.1 (SARS-CoV-2). Multiple sequence alignment was performed with ClustalO v.1.2.4 and visualized with MEGA X v.10.2.6 (https://www.megasoftware.net/). NCBI sequences of spike proteins from betacoronaviruses included in the analysis were as follows: SARS-CoV-2 (YP_009724390.1), RatG13 (bat) (QHR63300.2), PCoV (pangolin) (QIQ54048.1), SARS-CoV (YP_009825051.1), WIV16 (bat) (ALK02457.1), BtRl (bat) (QDF43815.1), Khosta-2 (bat) (QVN46569.1), MERS-CoV (YP_007188579.1), HKU5 (bat) (YP_001039962.1), MCoV (mouse) (AGT17716.1), HKU23 (camel) (QEY10673.1), BCoV (bovine) (AMQ23500.1), OC43 (YP_009555241.1), HKU24 (rat) (YP_009113025.1) and HKU1 (AXT92528.1).

Statistical analyses. Statistical analyses were performed using GraphPad Prism software v.9.2.0. Multiple group comparisons for plasma neutralization titres against a panel of SARS-CoV-2 pseudoviruses were applied using the Kruskal–Wallis test with false discovery rate method, and multiple testing correction was performed for each comparison using the Benjamini–Hochberg procedure at a 5% false discovery rate threshold. Factor change was calculated as the difference of geometric mean titre in the ID_{50} compared with that of the wild-type pseudotyped virus. Comparisons of neutralizing antibody responses by sex and smoke status were carried out using a paired Wilcoxon signed-ranked test. Correlation analysis between neutralizing antibody titres and age or BMI was carried out using Spearman's test. One-way analysis of variance (ANOVA) and Tukey's multiple comparison test were performed for statistical analysis of infectivity. A P value ≤ 0.05 was considered as statistically significant.

Ethical approval. The study protocol was approved by the Ethics Committee of the Faculty of Medicine at Universidad de Chile (project numbers 0361-2021 and 096-2020), Clínica Santa María (project number 132604-21) and CEC-Salud-UC (project number 200513023). All donors signed an informed consent, and their samples were anonymized.

Reporting Summary. Further information on research design is available in the Nature Research Reporting Summary linked to this article.

Data availability

Data are available in the Supplementary Information section. Source data are provided with this paper. Reagents used in this work will be available upon reasonable request to the corresponding authors.

Received: 4 August 2021; Accepted: 23 February 2022;
Published online: 1 April 2022

References

1. Harvey, W. T. et al. SARS-CoV-2 variants, spike mutations and immune escape. *Nat. Rev. Microbiol.* **19**, 409–424 (2021).
2. Tao, K. et al. The biological and clinical significance of emerging SARS-CoV-2 variants. *Nat. Rev. Genet.* **22**, 757–773 (2021).
3. *Tracking SARS-CoV-2 Variants* (WHO, 2021).
4. Romero, P. E. et al. The emergence of Sars-CoV-2 variant Lambda (C.37) in South America. *Microbiol. Spectr.* **9**, e0078921 (2021).
5. Khoury, D. S. et al. Neutralizing antibody levels are highly predictive of immune protection from symptomatic SARS-CoV-2 infection. *Nat. Med.* **27**, 1205–1211 (2021).
6. Earle, K. A. et al. Evidence for antibody as a protective correlate for COVID-19 vaccines. *Vaccine* **39**, 4423–4428 (2021).
7. Cromer, D. et al. Neutralising antibody titres as predictors of protection against SARS-CoV-2 variants and the impact of boosting: a meta-analysis. *Lancet Microbe* **3**, e52–e61 (2022).
8. Gilbert, P. B. et al. Immune correlates analysis of the mRNA-1273 COVID-19 vaccine efficacy clinical trial. *Science* **375**, 43–50 (2022).
9. Feng, S. et al. Correlates of protection against symptomatic and asymptomatic SARS-CoV-2 infection. *Nat. Med.* **27**, 2032–2040 (2021).
10. Mallapaty, S. China's COVID vaccines have been crucial – now immunity is waning. *Nature* **598**, 398–399 (2021).
11. Beltrán-Pavez, C. et al. Insights into neutralizing antibody responses in individuals exposed to SARS-CoV-2 in Chile. *Sci. Adv.* **7**, eabe6855 (2021).
12. Liu, Z. et al. Identification of SARS-CoV-2 spike mutations that attenuate monoclonal and serum antibody neutralization. *Cell Host Microbe* **29**, 477–488 e4 (2021).
13. Motozono, C. et al. SARS-CoV-2 spike L452R variant evades cellular immunity and increases infectivity. *Cell Host Microbe* **29**, 1124–1136 e11 (2021).
14. Weisblum, Y. et al. Escape from neutralizing antibodies by SARS-CoV-2 spike protein variants. *eLife* **9**, e61312 (2020).
15. McCallum, M. et al. N-terminal domain antigenic mapping reveals a site of vulnerability for SARS-CoV-2. *Cell* **184**, 2332–2347.e16 (2021).

16. González-Puelma, J. et al. Mutation in a SARS-CoV-2 haplotype from sub-Antarctic Chile reveals new insights into the Spike's dynamics. *Viruses* **13**, 883 (2021).
17. Yurkovetskiy, L. et al. Structural and functional analysis of the D614G SARS-CoV-2 spike protein variant. *Cell* **183**, 739–751.e8 (2020).
18. Mansbach, R. A. et al. The SARS-CoV-2 spike variant D614G favors an open conformational state. *Sci. Adv.* **7**, eabf3671 (2021).
19. Korber, B. et al. Tracking changes in SARS-CoV-2 spike: evidence that D614G increases infectivity of the COVID-19 virus. *Cell* **182**, 812–827.e19 (2020).
20. Polack, F. P. et al. Safety and efficacy of the BNT162b2 mRNA Covid-19 vaccine. *N. Engl. J. Med.* **383**, 2603–2615 (2020).
21. Liu, C. et al. The architecture of inactivated SARS-CoV-2 with postfusion spikes revealed by cryo-EM and cryo-ET. *Structure* **28**, 1218–1224 e4 (2020).
22. Gupta, D. et al. Inactivation of SARS-CoV-2 by beta-propiolactone causes aggregation of viral particles and loss of antigenic potential. *Virus Res.* **305**, 198555 (2021).
23. Haas, E. J. et al. Impact and effectiveness of mRNA BNT162b2 vaccine against SARS-CoV-2 infections and COVID-19 cases, hospitalisations, and deaths following a nationwide vaccination campaign in Israel: an observational study using national surveillance data. *Lancet* **397**, 1819–1829 (2021).
24. Jara, A. et al. Effectiveness of an inactivated SARS-CoV-2 vaccine in Chile. *N. Engl. J. Med.* **385**, 875–884 (2021).
25. Wang, M. et al. Reduced sensitivity of the SARS-CoV-2 Lambda variant to monoclonal antibodies and neutralizing antibodies induced by infection and vaccination. *Emerg. Microbes Infect.* **11**, 18–29 (2022).

Acknowledgements

We thank all volunteers for participating in this study. We also thank J. Catrileo (Universidad de Chile), D. Silva (Universidad de Chile), M. Peña (Universidad de Chile), M. A. Núñez and the blood bank staff members (Clínica Santa María), and M. Gilabert and the Clinical Data Management Unit (Clínica Santa María) for technical support and sample collection. We thank L. Nuñez for her critical revision. La Agencia Nacional de Investigación y Desarrollo (ANID) Chile provided support through Fondecyt grants numbers 1190156 (R.S.-R.), 1211547 (F.V.-E.), 1181656 (A.G.), 1180882 (M.A.N.) , 3200460 (A.B.) and through the ICM grant number ICN2021_045 (R.S.-R.). SECTEI/138/2019 from Mexico City to L.A.-P. N.L.C. is supported by ANID 0920, M.A.N. and M.M.d.O. are supported by Educación Superior Regional (ESR) grants MAG1995 and MAG2095 and M.F. is supported by Didemuc SC-11. This work was partially funded by FOCEM (MERCOSUR Structural Convergence Fund), COF 03/11, and the 'URGENCE COVID-19' fundraising campaign of Institut Pasteur (S.P.). The funding source had no role in the design of this study or its execution, analyses, interpretation of the data or decision to submit the results.

Author contributions

M.L.A., A.G.-A., C.P.C., A.G., F.V.-E. and R.S.-R. designed the study. M.L.A., L.A.-P. and A.B. designed the mutants and performed experiments with pseudotyped viruses. A.G., C.P.C., M.F. and N.L.C. provided the clinical samples. M.L.A., A.G.-A., F.P. and F.V.-E. performed the statistical analysis. M.M.d.O., S.P. and M.A.N. performed the structural and bioinformatic analyses. C.M.-V. and J.A. isolated all SARS-CoV-2 variants and performed infections at the BSL3 facility. F.V.-E. and R.S.-R. wrote the manuscript. F.V.-E., A.G. and R.S.-R. acquired the funding. All authors approved the final version of the manuscript.

Competing interests

The authors declare no competing interests.

Additional information

Extended data is available for this paper at https://doi.org/10.1038/s41564-022-01092-1.

Supplementary information The online version contains supplementary material available at https://doi.org/10.1038/s41564-022-01092-1.

Correspondence and requests for materials should be addressed to Fernando Valiente-Echeverría or Ricardo Soto-Rifo.

Peer review information *Nature Microbiology* thanks Olivier Schwartz, Natalia Laufer and the other, anonymous, reviewer(s) for their contribution to the peer review of this work. Peer reviewer reports are available.

Reprints and permissions information is available at www.nature.com/reprints.

Publisher's note Springer Nature remains neutral with regard to jurisdictional claims in published maps and institutional affiliations.

a

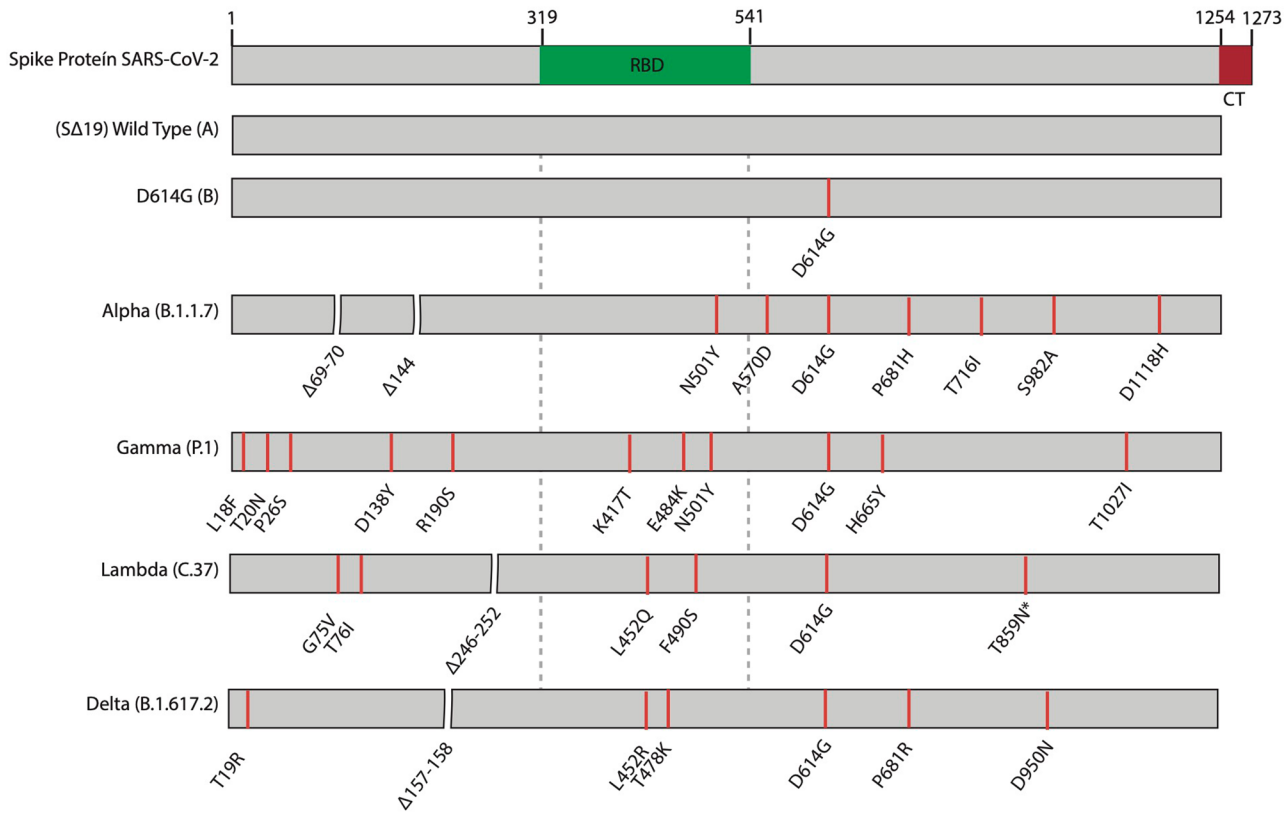

b

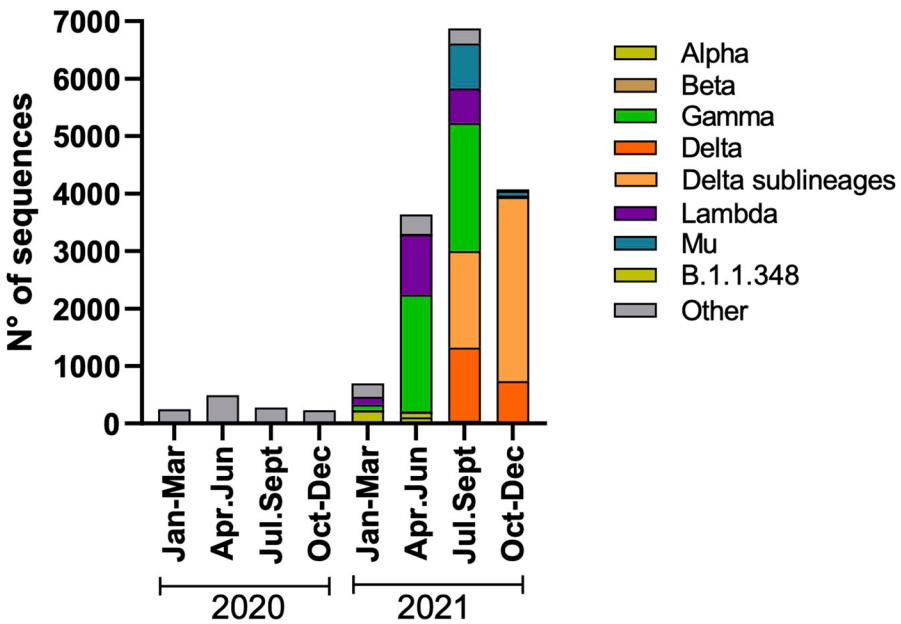

Extended Data Fig. 1 | See next page for caption.

Extended Data Fig. 1 | SARS-CoV-2 variants analyzed in this study. (**a**) Schematic representation of the SARS-CoV-2 spike protein and the variants used in this study. Lineages are indicated in parenthesis. RBD, receptor-binding domain, CM; cytoplasmic tail. (**b**) SARS-CoV-2 variants and lineages circulation in Chile according to public data deposited at https://auspice.cov2.cl/ncov/chile-global.

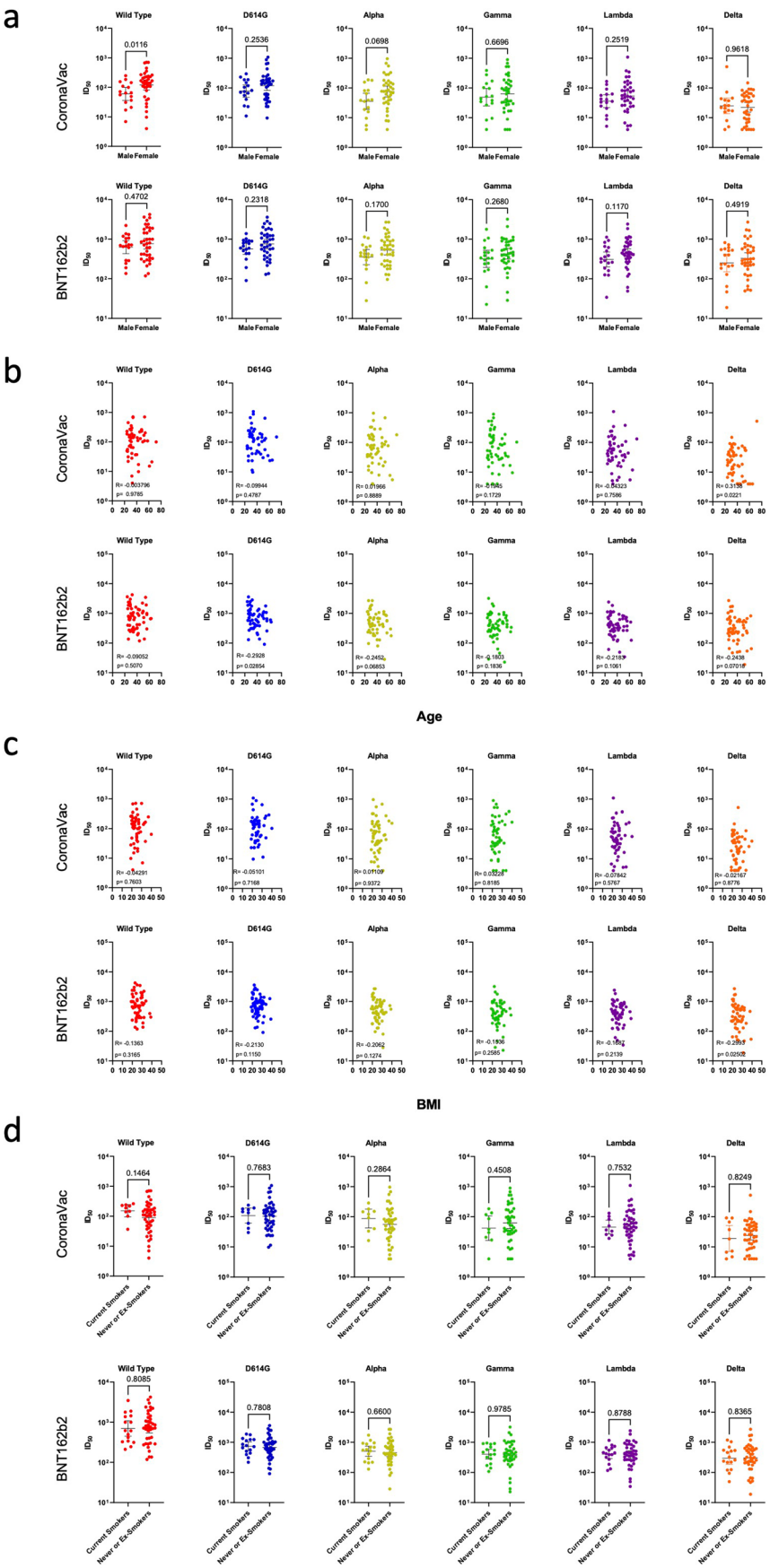

Extended Data Fig. 2 | See next page for caption.

Extended Data Fig. 2 | Correlation of neutralizing antibody titers against SARS-CoV-2 variants and vaccinated participants' sex, age, BMI or smoke status. Stratification neutralizing antibody titres (NAbTs) against SARS-CoV-2 variants by sex (**a**), age (**b**), BMI (**c**) and smoke status (**d**) for the CoronaVac group (n = 53) and the BNT162b2 group (n = 56). Comparisons of NAbs responses by sex (a) and smoke status (d) were carried out using a paired Wilcoxon signed-ranked test. A two tailed P value are shown. Correlation analysis between NAbs and age or BMI was carried out using Spearman's test; Spearman R and the corresponding two-tailed P values are shown in the botton left corner. A P value ≤0.05 was considered as statistically significant.

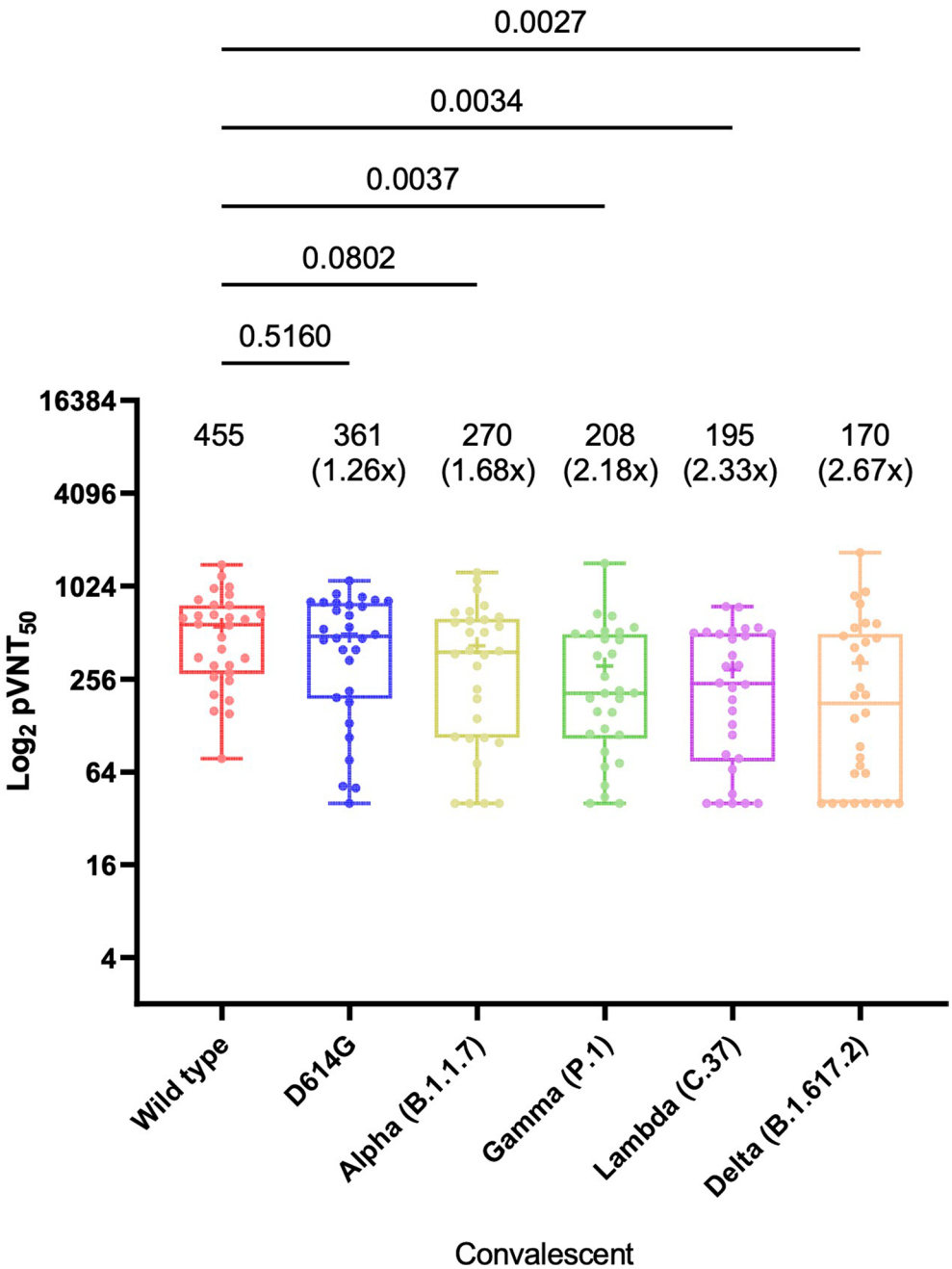

Extended Data Fig. 3 | Neutralization titers of plasma from convalescent individuals. 50% pseudovirus neutralization titers ($pVNT_{50}$) of convalescent individuals (n = 30) against SARS-CoV-2 pseudotype bearing the Wuhan reference strain (Wild Type) or lineage D614G, Alpha (B.1.1.7), Gamma (P.1), Lambda (C.37) and Delta (B.1.617.2) spike protein. Box plots indicated the median and interquartile range (IQR) of $pVNT_{50}$ for each SARS-CoV-2 pseudotype. Factor changes are shown in brackets as the difference of the geometric mean titer in the $pVNT_{50}$ as compared with that of the Wild type pseudotyped virus. Statistical analyses were performed with the two-tailed Kruskal–Wallis test after adjustment for the false discovery rate. GMTs are indicated.

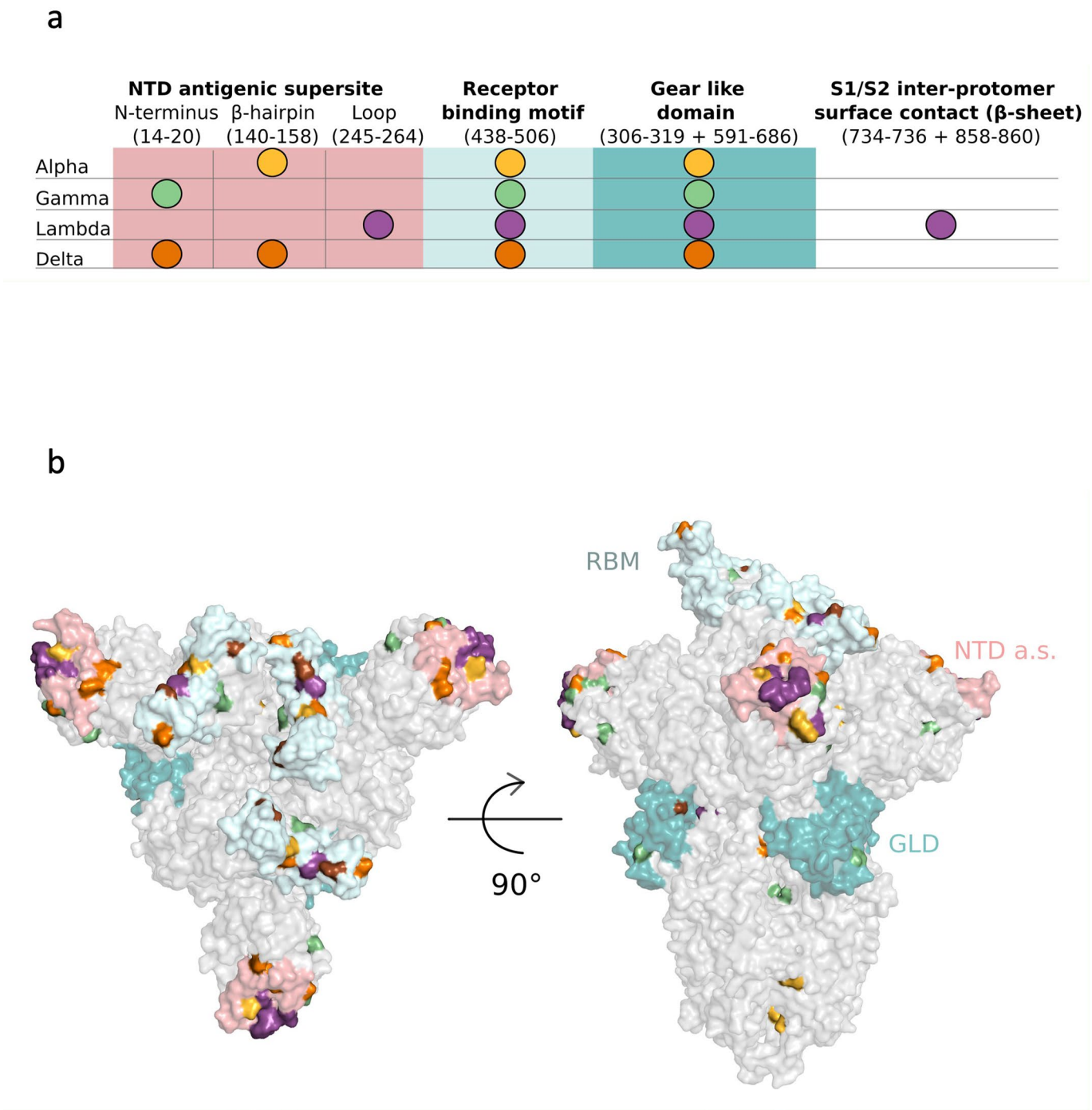

Extended Data Fig. 4 | Comparative analysis and location of the mutations in different SARS-CoV-2 variants. (**a**) Schematic representation of the different domains containing spike mutations. Color codes according to the variant correspond to that of Fig. 1. (**b**) Mapping of mutation sites on the spike structure (PDBid: 7BNN).

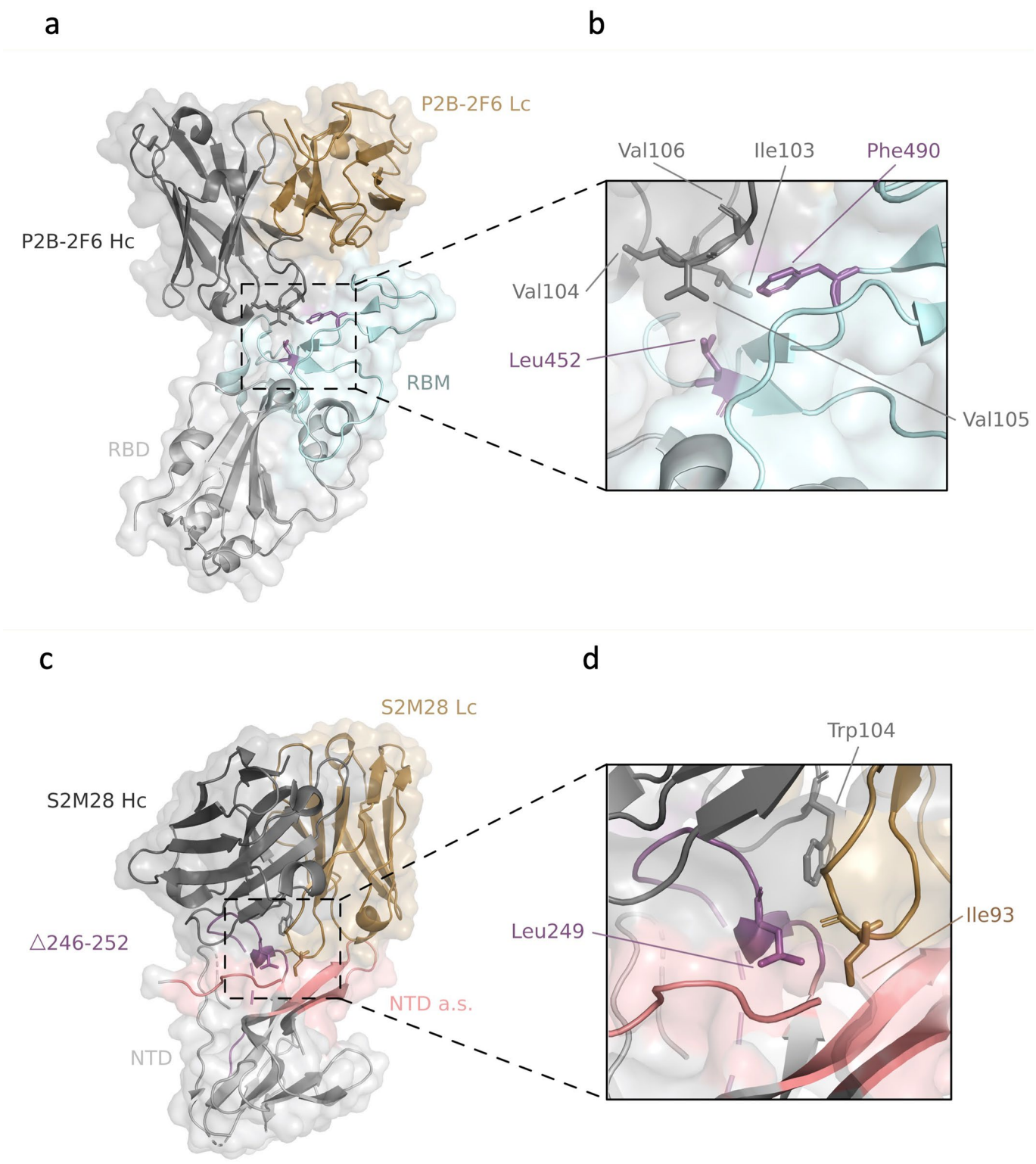

Extended Data Fig. 5 | Lambda mutations mapping on known antibody recognition epitopes. (**a**) X-ray structure (PDBid:7BWJ) of a complex between wild type RBD from SARS-CoV2 and the monoclonal antibody P2B-2F6, isolated from B-cells from an infected individual. **b**) Close up on the hydrophobic interactions established by L452 and F490 in the protein-protein interface. Mutations to polar amino acids as L452Q, F490S clearly disrupt the hydrophobic interface. **c**) Same as a) for antibody S2M28 solved by CryoEM (PDBid:7LY0), which recognizes the highly antigenic segment of the NTD domain. **d**) The close-up highlights the NTD-antibody interaction L249-I93. The deletion 246-252 would completely abrogate the binding by drastically reducing the binding epitope.

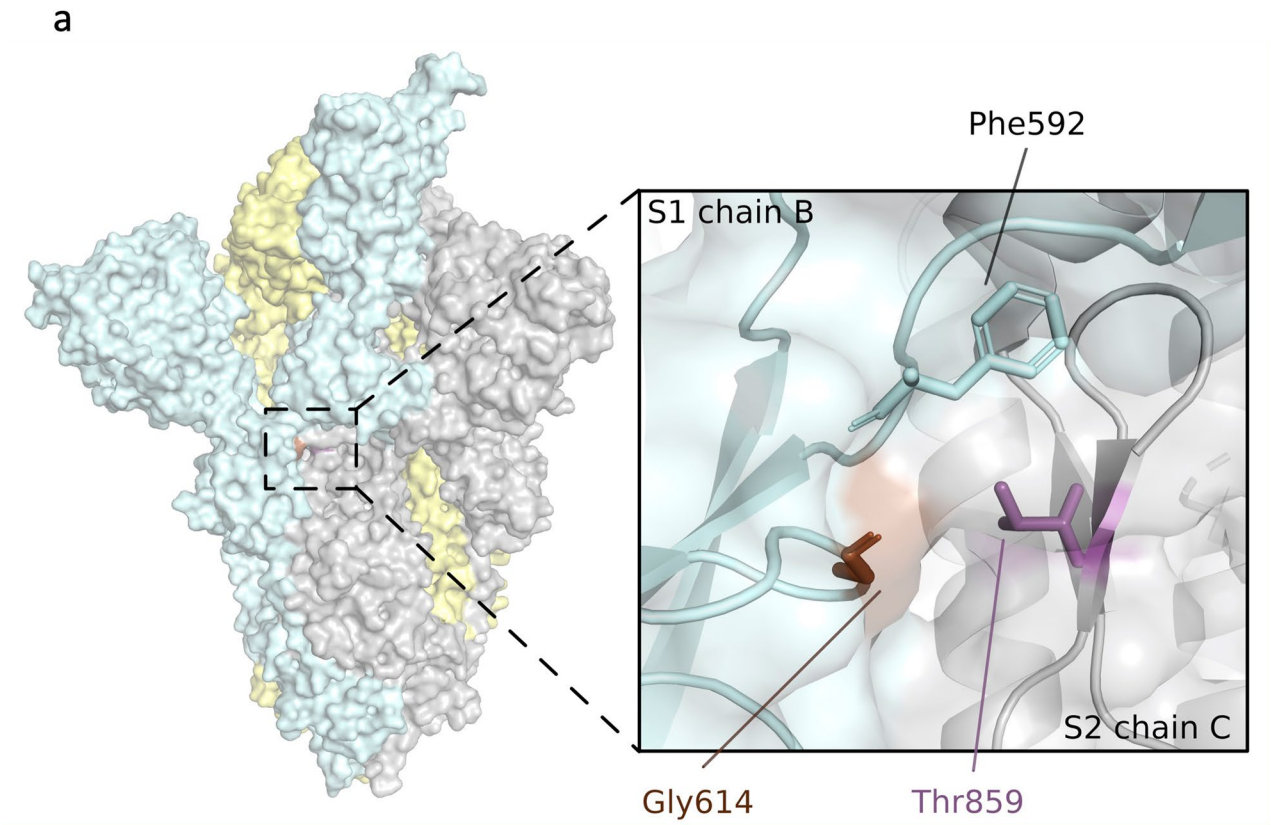

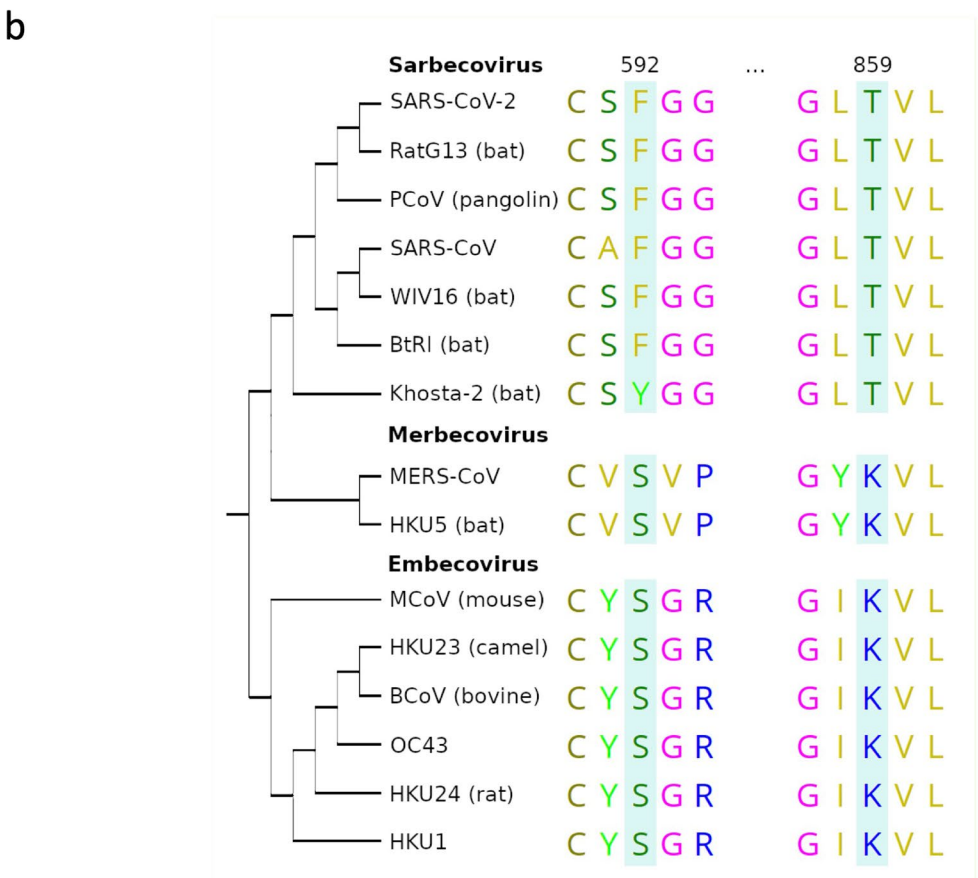

Extended Data Fig. 6 | See next page for caption.

Extended Data Fig. 6 | Multiple sequence alignment of betacovronaviruses around F592 and T859. (**a**) Insight on the neighborhood of T859 at the interface of two spike protomers. The inset on the right shows the hydrophobic interaction with F592 in the next protomer. G164 is also shown for reference. (**b**) The hydrophobic interaction between T859 and F592 is only possible in Sarbecovirus as other subgenera present a putatively correlated mutation at those positions (K and S, respectively).

nature portfolio

Corresponding author(s): Ricardo Soto-Rifo & Fernando Valiente-Echeverría

Last updated by author(s): 2022/02/03

Reporting Summary

Nature Portfolio wishes to improve the reproducibility of the work that we publish. This form provides structure for consistency and transparency in reporting. For further information on Nature Portfolio policies, see our Editorial Policies and the Editorial Policy Checklist.

Statistics

For all statistical analyses, confirm that the following items are present in the figure legend, table legend, main text, or Methods section.

n/a	Confirmed
☐	☒ The exact sample size (*n*) for each experimental group/condition, given as a discrete number and unit of measurement
☐	☒ A statement on whether measurements were taken from distinct samples or whether the same sample was measured repeatedly
☐	☒ The statistical test(s) used AND whether they are one- or two-sided *Only common tests should be described solely by name; describe more complex techniques in the Methods section.*
☐	☒ A description of all covariates tested
☐	☒ A description of any assumptions or corrections, such as tests of normality and adjustment for multiple comparisons
☐	☒ A full description of the statistical parameters including central tendency (e.g. means) or other basic estimates (e.g. regression coefficient) AND variation (e.g. standard deviation) or associated estimates of uncertainty (e.g. confidence intervals)
☐	☒ For null hypothesis testing, the test statistic (e.g. *F*, *t*, *r*) with confidence intervals, effect sizes, degrees of freedom and *P* value noted *Give P values as exact values whenever suitable.*
☒	☐ For Bayesian analysis, information on the choice of priors and Markov chain Monte Carlo settings
☒	☐ For hierarchical and complex designs, identification of the appropriate level for tests and full reporting of outcomes
☐	☒ Estimates of effect sizes (e.g. Cohen's *d*, Pearson's *r*), indicating how they were calculated

Our web collection on statistics for biologists contains articles on many of the points above.

Software and code

Policy information about availability of computer code

Data collection	No codes were used to collect the data in this study
Data analysis	- Statistical analyses were performed using GraphPad Prism software version 9.2.0. - Structural alignments were performed using Swiss-PdbViewer, displayed by PyMOL v.2.4.1 (http://www.pymol.org/pymol), and rendered by Blender v.2.92.0 (http://www.blender.org) - Multiple sequence alignment was performed with ClustalO v1.2.4 and visualized with MEGA X v10.2.6

For manuscripts utilizing custom algorithms or software that are central to the research but not yet described in published literature, software must be made available to editors and reviewers. We strongly encourage code deposition in a community repository (e.g. GitHub). See the Nature Portfolio guidelines for submitting code & software for further information.

Data

Policy information about availability of data

All manuscripts must include a data availability statement. This statement should provide the following information, where applicable:

- Accession codes, unique identifiers, or web links for publicly available datasets
- A description of any restrictions on data availability
- For clinical datasets or third party data, please ensure that the statement adheres to our policy

Datasets are available in the Supplemental material section. Reagents used in this work will be available upon reasonable request to the corresponding authors.

Field-specific reporting

Please select the one below that is the best fit for your research. If you are not sure, read the appropriate sections before making your selection.

☒ Life sciences ☐ Behavioural & social sciences ☐ Ecological, evolutionary & environmental sciences

For a reference copy of the document with all sections, see nature.com/documents/nr-reporting-summary-flat.pdf

Life sciences study design

All studies must disclose on these points even when the disclosure is negative.

Sample size	The sample size was based on sample availability
Data exclusions	Participants with previous COVID-19 infection were excluded
Replication	Neutralization assays were performed once in technical duplicate. Infectivity assays were performed in technical triplicate for whole SARS-CoV-2 and in technical triplicates along three independent experiments for infections with pseudotyped viruses. All replication assays were succesful.
Randomization	There was no randomization. However, plasma samples were classified in three groups according to the vaccine received by the donor (CoronaVac or BNT162b2) or whether they were convalescent.
Blinding	Since sample groups (CoronaVac, BTN162b2 or convalescent) required a different starting dilution (1:2; 1:5 or 1:20, respectively) and were analyzed with different pseudotyped viruses, investigators were not blinded when performing neutralization assays.

Reporting for specific materials, systems and methods

We require information from authors about some types of materials, experimental systems and methods used in many studies. Here, indicate whether each material, system or method listed is relevant to your study. If you are not sure if a list item applies to your research, read the appropriate section before selecting a response.

Materials & experimental systems

n/a	Involved in the study
☒	☐ Antibodies
☐	☒ Eukaryotic cell lines
☒	☐ Palaeontology and archaeology
☒	☐ Animals and other organisms
☐	☒ Human research participants
☒	☐ Clinical data
☒	☐ Dual use research of concern

Methods

n/a	Involved in the study
☒	☐ ChIP-seq
☒	☐ Flow cytometry
☒	☐ MRI-based neuroimaging

Eukaryotic cell lines

Policy information about cell lines

Cell line source(s)	HEK293T and HEK293T-ACE2 cells previosuly described from our laboratory (DOI: 10.1126/sciadv.abe6855). Vero-E6 were from Dr. Marcela Ferrés Laboratory (ATCC CRL-1586).
Authentication	HEK293T and HEK293T-ACE2 cells were authetified by Western blot against ACE2
Mycoplasma contamination	Cells lines are weekly tested for mycoplasma contamination and only micoplasma-free cells were used.
Commonly misidentified lines (See ICLAC register)	No commonly misidentified cell lines were used in this study

Human research participants

Policy information about studies involving human research participants

Population characteristics	Complete information provided in Supplementary Table 1
Recruitment	Health care workers without prior diagnosed SARS-CoV-2 infection from two sites in Santiago, Chile, were invited to participate. Volunteers received the two-doses scheme of CoronaVac or BNT162b2, each dose being administered 28 or 21 days apart, respectively, according to the Chilean vaccination program. Plasma samples were collected between May and

	June 2021. Convalescent individuals were participating in the study COVID0920. All participants signed an informed consent before any study procedure was undertaken. The only self-selection bias was applied to some samples based on the volume available to perform neutralization assays. Since this bias is related to the availabiltiy of the sample and not its neutralizing capacity, it is not expected to impact the results.
Ethics oversight	The study protocol was approved by the Ethics Committee of the Faculty of Medicine at Universidad de Chile (Projects Nº 0361-2021 and Nº 096-2020), Clínica Santa Maria (Project Nº132604-21) and CEC-Salud-UC (Project Nº 200513023). All donors signed an informed consent, and their samples were anonymized.

Note that full information on the approval of the study protocol must also be provided in the manuscript.